ORIGINAL ARTICLE

Electronic Structure, Optical Properties and Quantum Chemical Investigation on Synthesized Coumarin Derivative in Liquid Media for Optoelectronic Devices

A. G. Pramod[1] · C. G. Renuka[1] · Y. F. Nadaf[2] 🆔

Abstract

The newly synthesized 3,3′-((3-bromo-4-methoxyphenyl)methylene)bis(4-hydroxy-2H-chromen-2-one) (3-BMH) derivative have been investigated in a selected number of organic solvents having different polarity and refractive index at room temperature. From the absorption and emission spectra of the synthesized derivative in studied solvents showed bathochromic shift in both the cases (Uv-vis and emission spectra), the ground state dipole moment (μ_g) and excited state dipole moment (μ_e) were obtained by implementing [Chamma-Kwaski-Villate, Bakhshiev, Lippert-Mataga, McRay and Suppan] solvatochromic shift techniques depending on solvent polarity parameters. The larger dipole moment value is observed in the excited state as compared to the ground state dipole moment and this discrepancy in the dipole moment value is due to polar nature of the molecule. From the results of both experimental and theoretical energy gap is found to 3.14 eV in average, from this, it can be concluded that the 3-BMH molecule showed a good agreement with the semiconducting material bandgap so that the 3-BMH molecule can be used as a potential material for the optoelectronic application. Also, from results of quantum chemical studies, the electrostatic potential maps studies reveal the molecule is how much stable it describes the defining reactivity of the molecule towards positively and negatively charged reactants, size, shape, the location of nucleophilic and electrophilic sites. Further, the optoelectronic properties were investigated the CIE, CRI, color purity and CCT results of the 3-BMH in all studied solvents revels that this compound exhibits blue emission (National television standard committee system (NTSC) for the ideal blue chromacity coordinate 0.14, 0.08) and from the CIE results show the color emission of the molecule in order to design the desired OLED device application.

Keywords Hypsochromic · Dipole moment · Energy gap · Potential maps · Opto-electronic

Introduction

In the recent past, there is an endless demand for novel organic molecules, for the high-technology industry, nonlinear devices and in the field of biological sciences.

In view of this, coumarin dyes have received special substantial attention of the research community because of their potential role in anticoagulants, HIV inhibitors, pharmaceutical agents like anti-inflammatory and antioxidant agents, also due to long spectral range, enhanced fluorescence quantum yields, photostability, and good solubility in the safest solvents [1, 2]. Nevertheless, for physiological and enzymatic measurements, these dyes were used as fluorescent labels, pigments and as fluorescent probes [2]. Further, among coumarin derivatives, dimeric coumarins biscoumarins are the ones which occupy a fascinating position and these exist naturally in numerous micro-organisms and in plants extracts [2]. Nonetheless, biscoumarins have drawn good

✉ C. G. Renuka
   renubub@gmail.com

1   Department of Physics, Jnanabharathi Campus, Bangalore University, Bengaluru, India

2   Department of Physics and Material Research Centre, Maharani Science College for Women Bengaluru, Bengaluru, India

potential interest in recent years due to their versatile medical and biological application viz., anticancer, anti-bacterial, anti-inflammatory and antioxidant agents and many more [3–5]. In addition, these dyes can strongly exhibit tubulin aggregation also played an important role against cancer [6, 7]. Also, it has been reported that [8], the biscoumarin dyes showed excellent optical properties [9].

The effect of solvents should be understood in depth intending to understand and to determine the performance of electronic devices in different media. Their molar absorption coefficient was much larger than that of monocoumarins, and also their linear absorption and emission spectra were red-shifted, whilst their fluorescence quantum yield was high [10, 11]. Therefore, biscoumarin compounds are of great interest in the field of fluorescent dyes. In view of this, organic compounds consisting of (D-π-A) donor π acceptor functionality are of great interest for enhanced NLO property, high emission yield and of course several properties of the dye in solution mainly depend on the nature of their corresponding solvents environment. The increase of optical response in organic molecules is not only due to a high level of π conjugated charge transfer but it is also the increase in the conjugation length which plays an essential determining role in the delocalization of π electrons under light excitation [11–13].

The specific solute-solvent interactions viz., hydrogen bonding, donor-acceptor interactions and/or non-specific interactions such as polar and Vander Walls interactions are generally responsible for the solvent-dependent spectral shifts, knowledge of the impact of both types of solute-solvent interactions plays a very substantial role in analyzing the solvent effects [10, 14, 15]. The solute-solvent polarity, as well as the polarizability, performs a vital role in solute spectral properties. Effect of the solvent is related closely to the degree and nature of intermolecular solute-solvents interactions. Optical absorption and emission studies reveal that solute-solvent interactions can be best described from the intensity of the spectrum, shape, and wavelength. In recent days, the effect of solvents on excitation and emission characteristics has become a subject of extensive research [16–18]. Furthermore, the knowledge of excited state dipole moment of molecule is very much useful in providing the valuable information in designing nonlinear optical materials and geometrical and electronic structure of the molecule in the short-lived excited state, for a chromophore as a function of polarity of the medium, the tunability range of emission energy can also be evaluated using excited-state dipole moment [19–21].

Different methods namely stark splitting, electric-dichroism, electronic polarization of fluorescence and microwave conductivity are available in the literature for the determination of dipole moments in the excited-state, but the use of those methods are limited since those methods are equipment sensitive and also related to a very simple molecule. Nevertheless, the solvatochromic method is simpler and accurate compared above mention methods and also it gives a straight measure of the distribution of electrons in the molecule, photons causing excitation of electrons in a molecule resulting the charge distribution takes place which leads to a conformational change in the excited state [22–24]. Many of the researchers have intensively reported for the determination of ground and excited state dipole moments experimentally and theoretically, in different types of organic fluorescent compounds like indoles, purines, thiadiazole Nile red dyes, phloroglucinol, quinolones, coumarins, excite dyes, laurdan, badan, benzimidazolone, chalcones [25–28] etc.

Further, the organic semiconducting materials (OSCs) have received the potential application in designing of hybrid and organic electronic devices such as organic field effect transistors (OFETs), organic light emitting devices (OLEDs), and organic photovoltaic cells (OPVs) [29, 30]. Therefore, the semiconducting properties of OSCs and the relationship in-between molecular and supramolecular structures have become one of the important findings [31] over the past years moreover, most of them are concerning the evaluation of band gap of OSCs. In view of this, the energy gap (E_g) defines the separation (energy) between the lowest unoccupied molecular orbital (LUMO) to highest occupied molecular orbital (HOMO) for OSCs which is analogs to valance band and conduction band in inorganic semiconductors respectively [32, 33]. This knowledge of the Eg is one of the important parameters in designing organic electronic materials. The dipole moment of the molecule will also play a major role in determining the band gap of the molecule because of the polarity effect. Since the Eg of the organic molecule is determined by both theoretically and experimentally [34, 35]. The quantum chemical investigation was also performed in order to determine the chemical reactivity of the molecule in a vacuum and in acetone solvent.

Hence, in the present work involves the systematic investigation of optical (absorption and emission), dipole moment (using solvatochromic method) of synthesized 3-BMH compound dissolved in a suitable solvent. The optical property (band gap) experimentally and using Gaussian 09 W software theoretically of

the molecule, MEP, SAS and TED calculation were also discussed in this article from the result we can observe that the obtained band gap is in good agreement with inorganic semiconducting material which can be used for designing optoelectronic devices. In this regard we made an attempt in order to develop an OLED exhibiting property for our molecule for this, the CIE color coordinates, color purity, CRI, and other parameters were estimated by using the software.

Synthesis and Experimental Techniques

Synthetic Route for 3-BMH

The 3-BMH molecule was synthesized by using a mixture of 4-hydroxycoumarin (2 equivalent) and 1-Bromo-2-methoxybenzene (1 equivalent) taken in a 100 ml round bottom flask to this 10 ml of acetic acid is added, this mixture was refluxed for 3 h. The progress of the reaction was monitored by TLC (Eluent: EtOAc and n-hexane). The evaporation of the solvent in vacuum afforded the crude product which was recrystallized from acetic acid to get 3-BMH in 94% yield, the reaction scheme of 3-BMH is presented in Fig. 1.

Solvents

The spectroscopic grade solvents viz., methanol, acetone, cyclohexane, 1,4-dioxane, hexadecane, propanol, dimethyl sulfoxide, ethyl acetate, and ethanol were procured from SD Fine chemicals and used without further purification (the purity of all solvents is of 99.9%). The samples were prepared using these solvents and the concentration of the solution was maintained for about 10^{-5} to 10^{-6} mM because of self-aggregation and inner filter effects.

Characterization of Synthesized 3-BMH Compound

The linear absorption spectra were recorded using Perkin Elmer Lambda–35 UV–Vis spectrometer operating in the range of 200–1100 nm equipped with a deuterium and halogen lamps with a resolution of ±1 nm at room temperature. The fluorescence spectra were collected at room temperature with the help of Hitachi F-2000 fluorescence spectrophotometer operating in the range of 220–800 nm with a resolution of ±1 nm having a light source of 150 W Xenon lamp. The absorption and fluorescence measurements were repeated for several times and the spectra were consistent at all the times and also the instruments were well calibrated before the scan. The fluorescence lifetime was recorded using (TCSPC) Time-Correlated Single Photon Counting technique (Edinburgh Instruments, Model: FSP920) along with a Hamamatsu PMT detector.

Computational Method

Density Functional Theory (DFT) measurements were performed keeping Becke's 3 Lee-Yang-Parr/6–311(d) (DFT-B3LYP/6–311(d)) basic set using Gaussian 09 W program package software [36] the 3-BMH is optimized (ground state) in vacuum phase. Highest Occupied Molecular Orbital (HOMO), Lowest Unoccupied Molecular Orbital (LUMO) plots, energy levels and HOMO LUMO energy band gaps (E_g), and the electrostatic energy potential maps were also constructed in studied solvents using DFT-B3LYP/6–311(d) basic set. The basis set 6-31G(d,p) augmented by 'd' polarization function on heavy atom and 'p' polarization func-tion on hydrogen atoms were used for better description of polarbonds of molecules. It should be emphasized that 'p' polar-ization functions on hydrogen atoms useful not only for reproduc-ing the out-of-plane vibrations involv-ing hydrogen atoms are butalso for a better description of the molecular geometry and othernormal vibration modes.

Theoretical Background and Calculations

Despite different assumptions and theories (resulting in the same expression for Stokes shift) available in

Fig. 1 Reaction scheme for synthesis of 3-BMH
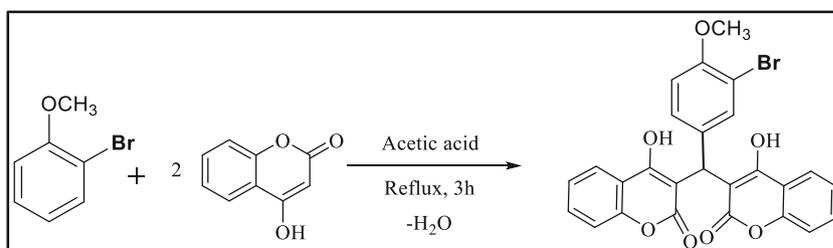
the literature, we adopted the solvatochromic method to estimate the ground state (μ_g) and excited singlet state (μ_e) dipole moments because of its simplicity in arriving the results. And in this method, the solvatochromic relations have been estimated by implementing the simplest quantum-mechanical second-order perturbation theory and by considering the Onsager reaction field for a polarizable dipole into account [37].

Chamma-Kwaski-Villate equation [38–40].

$$\frac{\nu_a + \nu_f}{2} = -q1\ F1\ (D, n) + constant \tag{1}$$

Bakhshiev's equation [41].

$$\nu_a - \nu_f = q_2\ F_2(D, n) + constant \tag{2}$$

Lippert's equation [42]

$$\nu_a - \nu_f = q_3\ F_3(D, n) + constant \tag{3}$$

McRae's equation [43]

$$\nu_a = -q_4\ F_4(D) + Constant \tag{4}$$

Suppan's equation [44]

$$\nu_a = -q_5\ F_5(D) + Constant \tag{5}$$

The relations F_1 (D, n) (Viallet's-Chamma-Kawski polarity relation), F_2 (D, n) (Bakhshiev's polarity relation), F_3 (D, n) (Lippert's polarity relation), F_4 (D) (McRae's polarity relation) and F_5(D) (Suppan's polarity relation) are listed below.

$$F_1(D, n) = \left[\frac{2n^2 + 1}{2(n^2 + 2)}\left(\frac{D-1}{D+2} - \frac{n^2-1}{n^2+2}\right) + \frac{3(n^4-1)}{2(n^2+2)^2}\right] \tag{6}$$

$$F_2(D, n) = \frac{2n^2 + 1}{n^2 + 2}\left[\frac{D-1}{D+2} - \frac{n^2-1}{n^2+2}\right] \tag{7}$$

$$F_3(D, n) = \left[\frac{D-1}{2D+1} - \frac{n^2-1}{2n^2+1}\right] \tag{8}$$

$$F_4(D) = \left[\frac{2(D-1)}{D+2}\right] \tag{9}$$

$$F_5(D) = \left[\frac{2(D-1)}{2D+2}\right] \tag{10}$$

Here, ν_a and ν_f are excitation and emission maxima are in wavenumbers (cm^{-1}). 'n' and 'D' are refractive index and dielectric constants of the solvents respectively. Now, plotting the graphs for the above

equations i.e., $\frac{\nu_a + \nu_f}{2}$ v/s $F_1(D, n)$, $\nu_a - \nu_f$ v/s $F_2(D, n)$, $\nu_a - \nu_f$ v/s $F_3(D, n)$, ν_a v/s $F_4(D)$ and ν_a v/s $F_5(D)$ should results in linear graphs with slopes q_1, q_2, q_3, q_4, and q_5 respectively are listed below.

$$q_1 = \frac{2\left(\mu_e^2 - \mu_g^2\right)}{hca^3} \tag{11}$$

$$q_2 = \frac{2\left(\mu_e - \mu_g\right)^2}{hca^3} \tag{12}$$

$$q_3 = \frac{2\left(\mu_e - \mu_g\right)^2}{hca^3} \tag{13}$$

$$q_4 = \frac{\mu_g\left(\mu_e - \mu_g\right)}{hca^3} \tag{14}$$

$$q_5 = \frac{\mu_g\left(\mu_e - \mu_g\right)}{hca^3} \tag{15}$$

Where, μ_g and μ_e are ground state and excited state dipole moment of solute molecules, 'h' and 'c' are Planck's constant and velocity of light in vacuum respectively. 'a' is Onsager cavity radius of a solute molecule obtained by according to Edward atomic increment method [45]. By assuming the fact that the ground state and excited state dipole moments are almost parallel to one another, the following relations are used to determine the dipole moments

$$\mu_g = \frac{q_1 - q_2}{2}\left[\frac{hca^3}{2q_2}\right]^{\frac{1}{2}} \tag{16}$$

$$\mu_g = \frac{q_1 + q_2}{2}\left[\frac{hca^3}{2q_2}\right]^{\frac{1}{2}} \tag{17}$$

$$\mu_e = \left[\frac{q_2 + q_3}{q_3 - q_2}\right]\mu_g; q_2 > q_3 \tag{18}$$

To derive for optoelectronic applications, the evaluation of mass extinction coefficient (α_{mass} Lg^{-1} cm^{-1}) at a given wavelength the light absorbed per unit mass density of the compound are important parameters and which are given by the equations [46].

$$\alpha_{mass} = \varepsilon / M_w \tag{19}$$

$$\varepsilon = \frac{A}{b*c} \tag{20}$$

Here, 'ε' ($Lmol^{-1}$ cm^{-1}) is the molar extinction coefficient, 'A' is the absorption of light by the compound for a particular temperature, 'b' is the distance of light which travelled through the sample, 'c' is the concentration and 'M_w' molecular weight of the compound.

The optical band gap energy or the forbidden bandwidth of optical transition E_g depends on 'α' (cm^{-1}) absorption coefficient and '$h\nu$' (eV) photon energy is given by equation [37].

$$\alpha(h\nu) = P^*\left(h\nu - E_g\right)^{1/2} \tag{21}$$

Here, P^* is constant, and the allowed direct transition band gap is mentioned in Eq. 21.

The quantum yield (Φ) provides significant information about the excited state, radiationless transitions, and coupling of electronic to vibrational states [38–40]. However, it is also used to determine the appropriateness of laser media, sample purity, and chemical structure, the relative 'Φ' can be calculated by using Eq. 22.

$$\Phi = \frac{\Phi_s \, F_u (OD_s) n_u^2}{F_s (OD_u) n_s^2} \tag{22}$$

Where Φ_s is the quantum yield of the standard reference, F_u and F_s are the integrated areas under the curve of emission spectra of the unknown and standard sample, OD_u and OD_s are optical densities of the unknown and standard sample, and n_u and n_s are the refractive index of both unknown and standard sample. The decay rate constants such as radiative (k_r) and non-radiative (k_{nr}) constants were determined by using the equations, where τ_0 is the lifetime in (ns) [47, 48].

$$k_r = \frac{\Phi}{\tau_0} \tag{23}$$

$$k_{nr} = \frac{1}{\tau_0} - k_r \tag{24}$$

Results and Discussions

Influence of Solvents on Absorption and Fluorescence Properties of 3-BMH

The electronic absorption and emission spectra of the molecule in selected polar and nonpolar solvents at ambient temperature were recorded and given predictable evidence about solvation effect on the ground state (μ_g) and excited state (μ_e), all the spectroscopic solvent parameters and solvent polarity functions are summarized in Table 1 Fig. 2 shows the broad absorption spectra of the studied 3-BMH derivative in selected solvents having two bands, from which it is evident that the molecule excite between the range 331–341 nm and 346–355 nm (both are in UV region), these two bands are obtained due to intermolecular charge transfer (ICT)

transitions [49], and this range also attributed to the π to π^* transition which is occurred from $S_o \rightarrow S_1$ or $S_o \rightarrow S_n$ transitions depending polarity of the solvent used in the study. In Fig. 2., a small change in absorption maximum on varying the solvent polarity has been observed and is ascribed to some polar character in ground state [50]. However, it is also evident that in studied solvents the excitation spectra showed a blue shift due to the large degree of stabilizati0n of the ground state in polar environments [51]. Also due to the formation of hydrogen-bonded solvated clusters in-between protic solvents and probe molecule and the blue-shifted spectra is often reported in charge transfer systems [20].

The synthesized 3-BMH compound exhibited a broad emission band under 350 nm excitation wavelength as shown in Fig. 3. The fluorescence emission spectra of a synthesized compound which is solvent dependent and exhibited a broad peak. The emission band is located in the wavelength range ranging in between 380 and 500 nm and it has been assigned to $\pi \rightarrow \pi^*$ electronic transitions which are due to delocalization in aromatic rings and -OH group with the solvent, conjugation between the bridge, -OH···Br interactions were also participating in these transitions [49]. Hence it is worthwhile to assign the observed peaks to the $\pi \rightarrow \pi^*$ electronic transitions due to delocalization in the aromatic ring and conjugation bridge in the molecule also due to the solvent interaction and lone pair of electrons [50, 51].

From the fluorescence spectra (Fig. 3) of studied compound it clear that the fluorescence spectra suffer a bathochromic shift with an increase in the solvent polarity. The same kind of bathochromic shift of fluorescence spectra was observed for ip2 by sidir et al. [49] and for 6-MQ in their corresponding fluorescence spectra with an increase in solvent polarity [19]. The bathochromic shift of fluorescence spectra with solvent polarity indicating that basicity is increased in the compound and which further indicates the greater stabilization of excited state in polar solvents [52]. Further, from the absorbance spectra (Fig. 2) of examined 3-BMH molecule, it is very much clear that the absorption bands are showing the bathochromic shift with an increase in solvent polarity. This bathochromic (spectral) shift in both the cases (absorption and emission) is occurred by the stabilization of the molecule also due to the increase in the polarity of the solvents used through hydrogen bonding [53]. Further, the charge distribution is varied or disturbed in between the ground and excited state of the molecule because of strong intermolecular interactions with polar solvents in the excited state, which is one of the major aspect leading to the

Table 1 Solvent polarity parameters of 3-BMH in all studied solvents

| Solvents	(D)	(n)	$F_1(D, n)$	$F_2(D, n)$	$F_3(D, n)$	$F_4(D, n)$	$F_5(D, n)$
Cyclohexane	2.01	1.424	4.385	−0.004	−0.002	0.504	0.336
Hexadecane	2.04	1.427	4.402	0.001	0.010	0.515	0.342
1,4-Dioxane	2.21	1.420	4.799	0.043	0.021	0.575	0.377
Ethyl acetate	6.02	1.370	8.605	0.490	0.201	1.252	0.715
Propanol	20.1	1.383	10.744	0.778	0.274	1.729	0.905
Acetone	20.6	1.357	10.896	0.790	0.285	1.735	0.907
Ethanol	22.4	1.359	10.973	0.802	0.287	1.754	0.915
Methanol	32.6	1.326	11.495	0.855	0.309	1.827	0.940
Dimethyl sulfoxide	46.6	1.476	11.390	0.841	0.264	1.877	0.958

bathochromic shift with an increase in the polarity of the solvents. Nevertheless, the significant change in the emission band compared to absorption band signifies the molecule in the ground state is less polarized by the polar solvents. Hence, the solvents affectability can be implicit in terms of $\pi \rightarrow \pi^*$ transition with ICT intermolecular charge transfer, signifying that the nonbonding electrons are not involved in $n \rightarrow \pi^*$ transition [47, 54]. From Table 6, it can be seen that the μ_e values are varied significantly, which clearly suggest that the emission spectra are c0mparatively much sensitive to solvent-induced solute-solvent interactions and conformational difference related to that of excitation spectra, which confirms significant changes in the geometry of excited state (μ_e) compared to ground state (μ_g).

The 3-BMH in all solvents energy yield of fluorescence is less than unity because of Stoke's losses. This is further supported by more k_{nr} and fewer k_r values. The decay rate constants radiative (k_r) and non-radiative (k_{nr}) (Table 2) were calculated by using Eq.

(23 and 24), the emissive rate constants for 3-BMH in all studied solvents having different polarities clearly suggests more effective transient displacement of charges between the ground and excited state. Obtained results are strongly suggesting as the solvent polarity varies, the relative quantum yield also varies from 40 to 70%. The molar extinction and mass extinction coefficient considerably enhanced in all studied solvents for 3-BMH compound Table 2 This result confirms that the fluorescence emission of 3-BMH in excited energy states are strongly dependent on the solvent environment.

Estimation of Dipole Moments

To estimation the dipole moment in ground state (μ_g) and excited state (μ_e) of the synthesized derivative 3-BMH the solvent polarity functions $F_{1(CKV)}$ (D, n), $F_{2\,(BKS)}$ (D, n), $F_{3\,(L-M)}$ (D, n), $F_{4\,(McRay)}$ (D) and $F_{5\,(Suppan)}$ (D) was used based on solvatochromic shift methods, the slopes (q), correlation
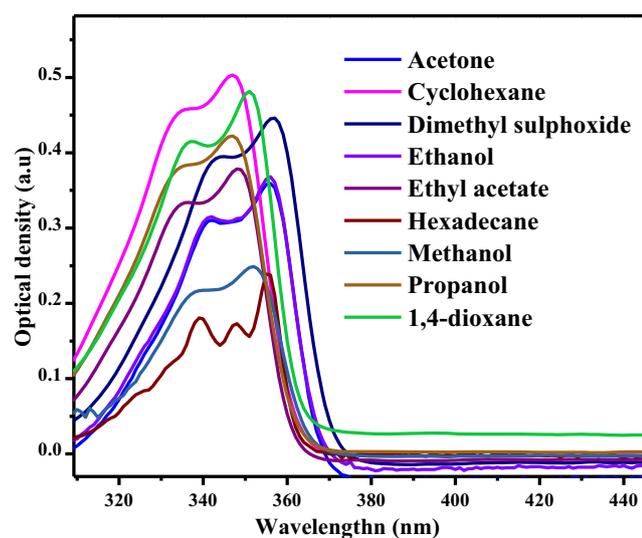

Fig. 2 UV-Vis absorption spectra of 3-BMH in all studied solvents
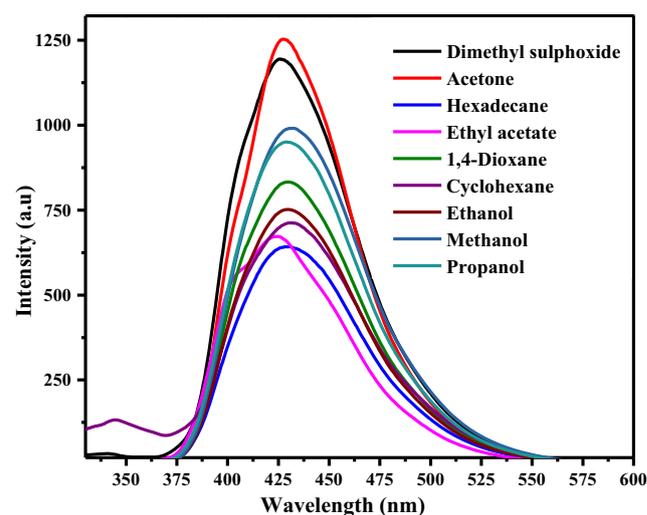
Fig. 3 Photoluminescence emission spectra of 3-BMH in all studied solvents

Table 2 Mass extinction coefficient (α_{mass}), molar extinction coefficient ($\varepsilon \times 10^4$), fluorescence quantum yield (Φ_F), fluorescence decay times (τ_0), radiative rate constant (k_r) and non-radiative rate constant (k_{nr}) in solvents with different refractive index 'n' and dielectric constant 'D'

Solvents	λ_{abs} (nm)	λ_{emi} (nm)	Stokes shift ($\Delta\lambda$)	α_{mass} (M^{-1} cm^{-1})	$\varepsilon \times 10^4$ (L mole^{-1} cm^{-1})	Quantum yield (Φ_F)	τ_0 (ns)	k_r (10^7 s^{-1})	k_{nr} (10^7 s^{-1})
Cyclohexane	347	428	81	3.85	2.01	0.40(±0.001)	1.2	33.4	49
Hexadecane	355	425	70	1.81	0.94	0.68(±0.001)	1.4	48.7	22
1,4-Dioxane	347	432	85	3.69	1.92	0.48(±0.001)	1.8	21.5	33
Ethyl acetate	356	430	74	2.91	1.51	0.51(±0.001)	1.7	29.3	29
Propanol	357	431	74	3.23	1.68	0.52(±0.001)	2.0	26.1	23
Acetone	348	429	81	2.75	1.43	0.69(±0.001)	1.9	36.6	15
Ethanol	356	431	75	2.82	1.47	0.45(±0.001)	1.5	30.4	36
Methanol	355	425	70	3.46	1.80	0.47(±0.001)	1.4	33.6	37
Dimethyl sulfoxide	356	430	74	3.38	1.76	0.70(±0.001)	1.9	36.8	15

coefficients and intercepts are derived by plotting $\frac{\nu_a+\nu_f}{2}$ vs. $F_{1(VCK)}$ (D, n) i.e., Chamma-Kwaski-Villate polarity, Stoke shift vs. $F_{2\,(BKS)}$ (D, n), Stoke shift vs. $F_{3\,(L-M)}$ (D, n), ν_a vs. $F_{4\,(McRay)}$ (D) and ν_a v/s. $F_{5\,(Suppan)}$ (D) (Figs. 4, 5, 6, 7, and 8 respectively, absorption and emission wavenumber data were presented in Table 3) and the slopes q_1, q_2, q_3, q_4 and q_5 (Eqns. 11–15) which are taken from these graphs respectively. The values such as correlation coefficient (R^2), slope (m), and intercept (z) were evaluated through linear fitting using origin software and all the values are summarized in Table 4, from which it is evident that the correlation coefficients found to be greater than 0.96 which indicates a good linearity of Stokes shift points. However, a small amount of deviation from linearity have been noticed in some solvents, it is due to specific solvent-solute interactions, and also probably due to hydrogen bonding nature of the molecule at the same instant time charge transfer in the excited state [55]. The μ_g and μ_e values estimated in the present investigation are in fair agreement with those estimated by different methods [56–58]. This difference

in the value of excited state dipole moment may be in part, due to assumptions and simplifications done in the solvatochromic method. As in Table 3 from which it is found that Stokes shift increased with increasing solvent polarity. The magnitude of Stokes shift represent that the excited state geometry could be significantly different from that of the ground state and thus large values of excited state dipole moments are expected. The obtained values of dipole moments are summarized in Table 5, and from which it is evident that, the value of μ_e is found to be more than μ_g. The differences in the ground and excited state dipole moment clearly reveal that, the investigated biscoumarin derivative is more polar in its excited state than in its ground state and which further concludes that solvent-solute interactions are significantly stronger in the excited state than in the ground state, explaining an essential redistribution of charge densities between both electronic states, the change in dipole moment on excitation reveals that because of hydrogen bonding effect and strong solvent polarity due to the possibility of the excited state is twisted intermolecular charge
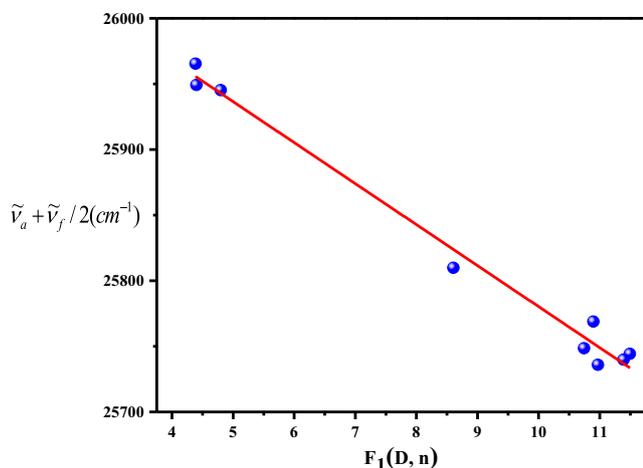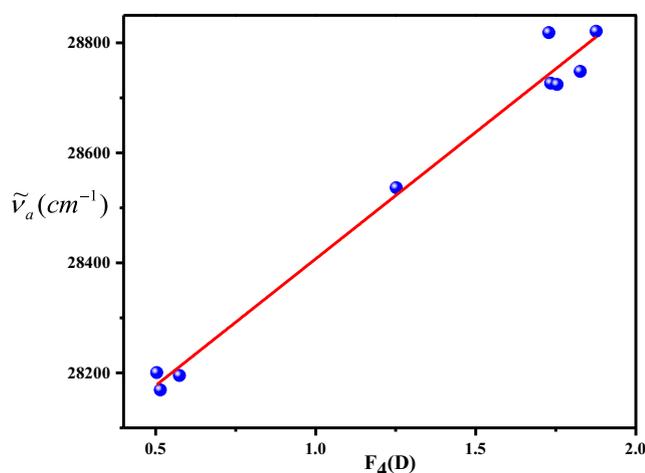
Fig. 4 A plot of $\frac{\nu_a+\nu_f}{2}$ function versus F_1 (D, n) of 3-BMH
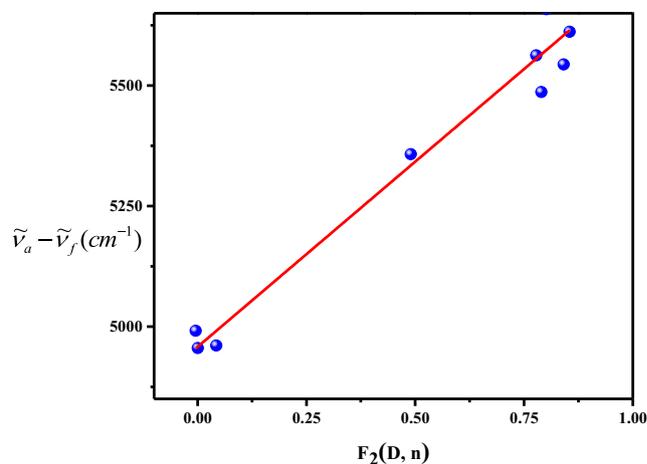
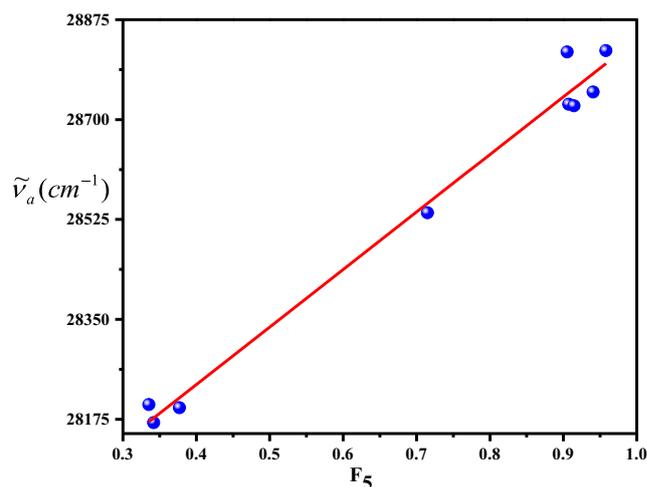**Fig. 5** A plot of $\nu_a - \nu_f$ function versus F_2 (D, n) of 3-BMH
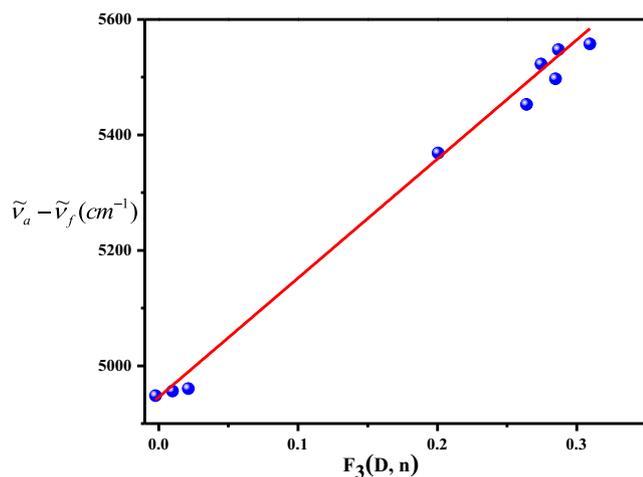
Fig. 6 A plot of $\tilde{\nu}_a - \tilde{\nu}_f$ function versus F_3 (D, n) of 3-BMH

Fig. 8 A plot of $\tilde{\nu}_a$ function versus F_5 (D) of 3-BMH

transfer in nature (TICT). Hence, due to large TICT molecule become polar as compared to ground state and change in dipole moment is observed.

The dipole moment was also calculated theoretically by using Gaussian 09 W program package software, in order to calculate the ground state dipole moment, the DFT-B3LYP/6–311(d) basic set is used whereas to calculate the excited state dipole moment, the TD-DFT-B3LYP/6–311(d) basic set is used. The synthesized derivative was optimized for both the basic set. From the observed results the obtained dipole moment (theoretical) is higher than the experimentally determined [59]. This discrepancy in dipole moment is because of organic molecules depends on the charge transfer process within the molecule, we found that the 3-BMH molecule is more polar in the excited state than the ground state. Therefore, the molecule is more sensitive to the solvent effect, this is perhaps due to some inherent circumstance of DFT formalism are responsible for this kind of inappropriate

outcome. Since, it is well understood that the DFT methods are not able to take care of week non-bonding interactions present in a particular system this moderates electron distribution of the model system and hence, electron density becomes significantly irregular [20, 60]. This features a virtual increase in polarity of the system, which is a path not quite the same as the original system. It is expected that a mixture of the method with a larger amount of electron correlation with higher order basic set, there is possible to improve in the figured dipole moment values. Whereas in case of considerably large molecules like 3-BMH the application of greater order method and considerably different size basic sets increases the computational cost effectively. Overwhelm, it is also found that the dipole moment of the molecule is affected by the solvent polarity used in this article.

Theoretical and Experimental Linear Optical Bandgap

Estimation of band gap from absorption measurements the result signifies a major role in the optoelectronic application. Higher the bandgap more tightly the valance electrons are bound to the nucleus. In this regard, the dependency of photon energy with an optical absorption coefficient is used to study the band structure and the type of transition involved. The optical band gap is determined by making use of the Tauc and Davis & Mott model [61] in the maximum absorption region. The general method for determining the bandgap to draw a plot of $(\alpha h\nu)^2$ $(cm^{-1}\ eV)^2$ versus 'hν' (eV) in solution phase are presented in Fig. 9. The linearity observed in the curves is shown by the arrows which confirm that the electronic transitions are direct allowed transitions. The E_g optical energy bandgap is estimated by means of extrapolating the linear region (Fig. 9). Hence, the calculated and measured bandgap E_g values are dissipated in Table 6. As we can conclude by observing Table 6 the experimental bandgap values of the studied molecule is found in the range between 3.37 to

Fig. 7 A plot of $\tilde{\nu}_a$ function versus F_4 (D) of 3-BMH

Table 3 The absorption and emission wavenumber data in different solvent medium of 3-BMH molecule

Solvents	ν_a (cm^{-1})	ν_f (cm^{-1})	$\nu_a - \nu_f$ (cm^{-1})	$\nu_a + \nu_f$ (cm^{-1})	$\nu_a + \nu_f/2$ (cm^{-1})
Cyclohexane	28818	23364	5454.0	52182.9	26091
Hexadecane	28169	23529	4639.6	51698.4	25849
1,4-Dioxane	28818	23148	5670.3	51966.6	25983
Ethyl acetate	28089	23255	4834.1	51345.7	25672
Propanol	28011	23201	4809.3	51213.1	25606
Acetone	28735	23310	5425.6	52045.7	26022
Ethanol	28089	23201	4888.0	51291.7	25645
Methanol	28169	23529	4639.6	51698.4	25849
Dimethyl sulfoxide	28089	23255	4834.1	51345.7	25672

3.44 eV [62]. Thus, the redshift in bandgap energy was observed by rising different solvents polarity. The degree of structural disorder and order was led to changes in E_g values and also which will change the distribution of energy levels within the energy gap [63]. Here, E_g values (Table 6) were shifted and it is found that the values are increasing or decrease (depend on dielectric constant, refractive index and viscosity) when the sample was exposed in the different solvent environment.

The theoretical band gap energy is calculated by using Gaussian 09 W software by implementing DFT-B3LYP/6-31G (d) basic set in ground state the calculated HOMO, LUMO energies and theoretical band gap energy were also dissipated in Table 6. The molecular orbitals of 3-BMH in one of studied acetone solvent are presented in Fig. 10 and the left of solvents such as cyclohexane, hexadecane, 1,4-dioxane, ethyl acetate, propanol, ethanol, methanol, and dimethyl sulphoxide HOMO, LUMO, and oscillator strength values are dissipated in Table 6 The orbital diagrams are plotted with the counter value of 0.02 a.u. peru color (Fig. 10) indicates positive and royal blue color indicates a negative value of the density distribution plots of HOMO and LUMO. This density distribution shows the typical π molecular orbital characteristics, from this analysis we infer that the lowest lying singlet to singlet absorption and electronic transition of $\pi \rightarrow \pi^*$ type. The HOMO and LUMO energies for acetone solvent are found to be −5.5167 eV and −1.6186 eV respectively. Hence, the HOMO-LUMO band gap is 3.898 eV. As we can see from the HOMO LUMO figures of acetone (Fig. 10), the HOMO is dominantly localized on 1-bromo-2-methoxybenzene group of the molecule along with some of the carbon and hydrogen atoms linked to this group because of −Br:-OCH$_3$ group present in the molecule. The LUMO is localized on almost all part of the molecule except the substituent group and the last benzene ring present in the parent group of the molecule. Hence, the molecular orbital densities HOMO and LUMO showed similar observations for all other studied solvents. Therefore, we can infer that the double bond has a maximum electron density distribution in the LUMO as compared to the HOMO [63]. The overall energy gap E_g was found in the range between 3.71 to 3.89 eV. Nevertheless, it is very much significant to point out that the obtained discrepancies in between theoretically and experimental obtained results can be ascribed due to the fact that the experimental results belonged to solution phase in which there are several inter- and intra-molecular interactions within the solvent and solution can be seen. Whereas, in case of theoretical calculations (using the software) it may belong to the solvent phase of an isolated single molecule. Thus, this bandgap (wide) and the optical transparency of the compound with the lower E_g can be especially preferred in the field of optoelectronics as a source of light emitting diodes and laser diodes.

Table 4 Statistical treatment of correlation of solvents spectral shifts of 3-BMH

Compound	Method	Slope (m)	Intercept (z)	Correlation coefficient (R^2)
3-BMH	Viallet's-Chamma-Kawski	−31.2434	26092	0.9858
	Bakhshiev's	768.222	4958	0.9542
	Lippert's	2063.56	4945	0.9681
	McRae	460.328	27946	0.9824
	Suppan	1007.78	27832	0.9832

Table 5 Ground and excited state dipole moment of 3-BMH

Compound (3-BMH)	Dipole moment (Debye)
μ_g^a	0.238
μ_g^b	0.127
μ_e^c	6.661
μ_e^d	1.254
μ_e^e	3.142
μ_e^f	4.897
μ_e^g	2.123
μ_e^h	3.015

Debye (D) = 3.33564×10–30 cm = 10-18 esu cm

[a] The ground states dipole moments calculated using Gaussian software

[b] The ground states dipole moments calculated using Eq. (16)

[c] The excited states dipole moments calculated using Gaussian software

[d] The experimental excited states dipole moments calculated from Chamma-Kwaski-Villate equation

[e] The experimental excited states dipole moments calculated from Bakshiev's equation

[f] The experimental excited states dipole moments calculated from Lippert's equation

[g] The experimental excited states dipole moments calculated from McRay equation

[h] The experimental excited states dipole moments calculated from Suppan equation

Electrostatic Potential Maps

The Electrostatic potential maps are an important tool in defining reactivity of the molecule towards positively or negatively charged reactants, also it provides knowledge about size, shape, the location of electrophilic, nucleophilic sites, polarity and charge density of molecule. The 3-Dimensional molecular, electrostatic and total density maps were constructed with DFT theory with DFT-B3LYP/6–311(d) basic set are shown in Fig. 11. Electron density plots studies were estimated in a vacuum and in all solvents used in this article, the obtained result showed the uniform distribution and here only the acetone solvent density plot is dissipated [52]. The total electron density plots are showed uniform distribution. An MEP is a very influential tool describes, the molecular sites of hydrogen bonding interaction, nucleophilic reactions, and electrophilic attack. By using 6-311G level theory we calculated the $\rho(r)$ - the molecular electrostatic potential surface is found that 5×10^{-5} electrons/bohr^3 contour of the total
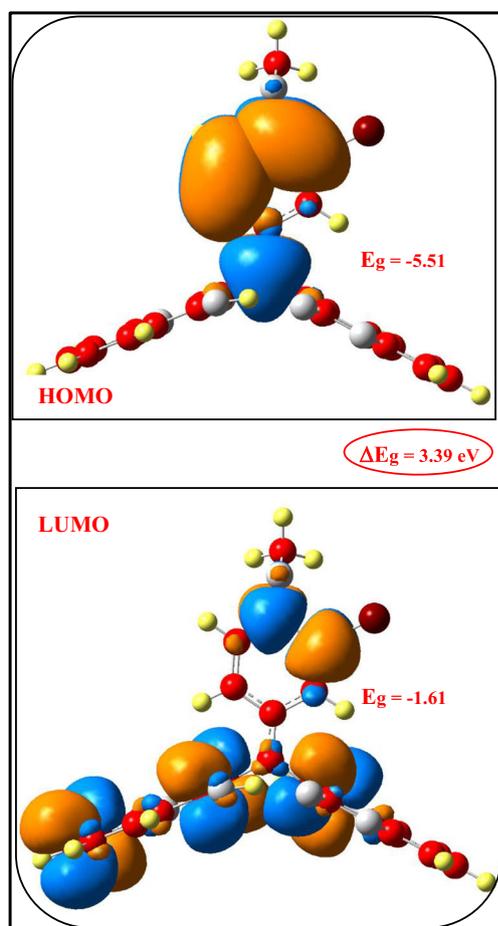
Fig. 9 Tau plot of 3-BMH in liquid media for all studied solvents
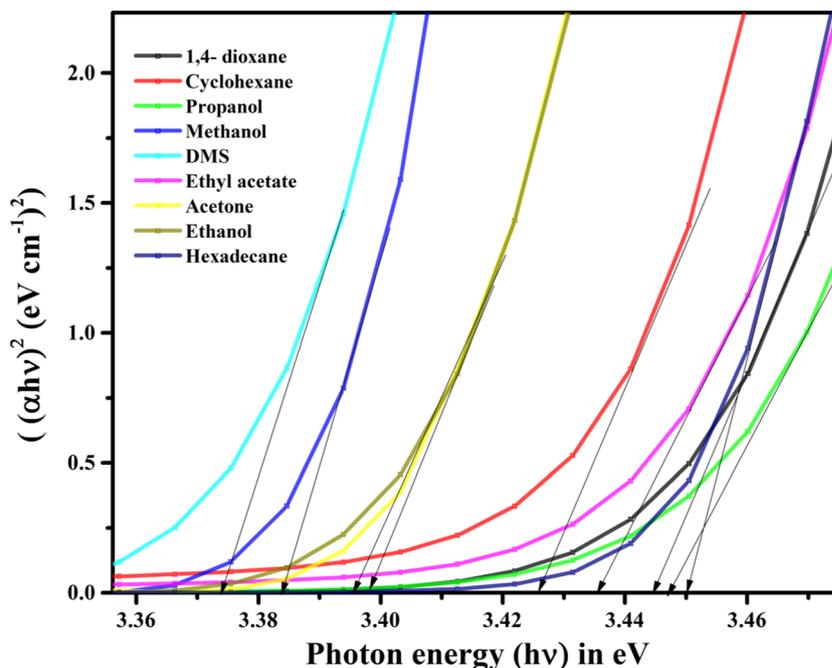
Table 6 Experimental and theoretical energy gap of 3-BMH in all studied solvents

Solvents	HOMO (eV)	LUMO (eV)	Band gap (eV)		Oscillator strength
			E_g(Theo)	E_g(Exp)	
Cyclohexane	−5.5988	−1.8988	3.711	3.422	0.797
Hexadecane	−5.5912	−1.7092	3.881	3.443	0.811
1,4-Dioxane	−5.5757	−1.7690	3.806	3.441	0.807
Ethyl acetate	−5.6355	−1.7636	3.871	3.431	0.790
Propanol	−5.6782	−1.7818	3.896	3.448	0.787
Acetone	−5.5167	−1.6186	3.898	3.394	0.789
Ethanol	−5.6268	−1.8735	3.753	3.392	0.765
Methanol	−5.5469	−1.7943	3.752	3.382	0.798
Dimethyl sulfoxide	−5.6026	−1.7965	3.806	3.371	0.789

self-consistent field (SCF) electron density for 3-BMH dye. In Fig. 11 the localized electron regions with electrostatic potential are red in color as negative, and green in color as positive distribution maps [18]. The negative MEP (red colour) region of high electron density which are mapped on 3C (E = −1.13 eV), 5C (E = −1.34 eV), 8C (E = −1.25 eV), 26O (E = −0.83 eV), and 29H (E = −1.08 eV) for in vacuum and at 2C (E = −0.93 eV), 4C (E = 1.46 eV), 14C (E = 1.16 eV), 15C (E = −1.48 eV), 39C (E = −0.81 eV), 41C (E = −1.03 eV), 42C (E = −0.69 eV), 49H (E = −1.01 eV), 52H (E = −1.48 eV), 23O (E = −0.48 eV), and 24O (E = −0.31 eV) in acetone solvent respectively. The positive MEP (green colour) regions of highly depleted electron density, which are mapped on these bounded atoms 11C-12C (E = 0.42 and 0.21 eV), 13C - 9C (E = 0.04 and − 0.11 eV), 10C - 7C (E = 0.26 and − 0.39 eV), 21C - 10C (E = −0.10 and − 0.08 eV), 35C - 19C (E = 0.21 and − 0.25 eV), 16C - 21C (E = −0.47 and − 0.11 eV), 38H - 45Br (E = −0.61 and − 0.66 eV), 44C - 46H (E = −0.62 and − 0.45 eV), 44C - 48H (E = −0.62 and − 0.02 eV), 44C - 47H (E = −0.48 and − 0.42 eV), in vacuum and in acetone solvent.
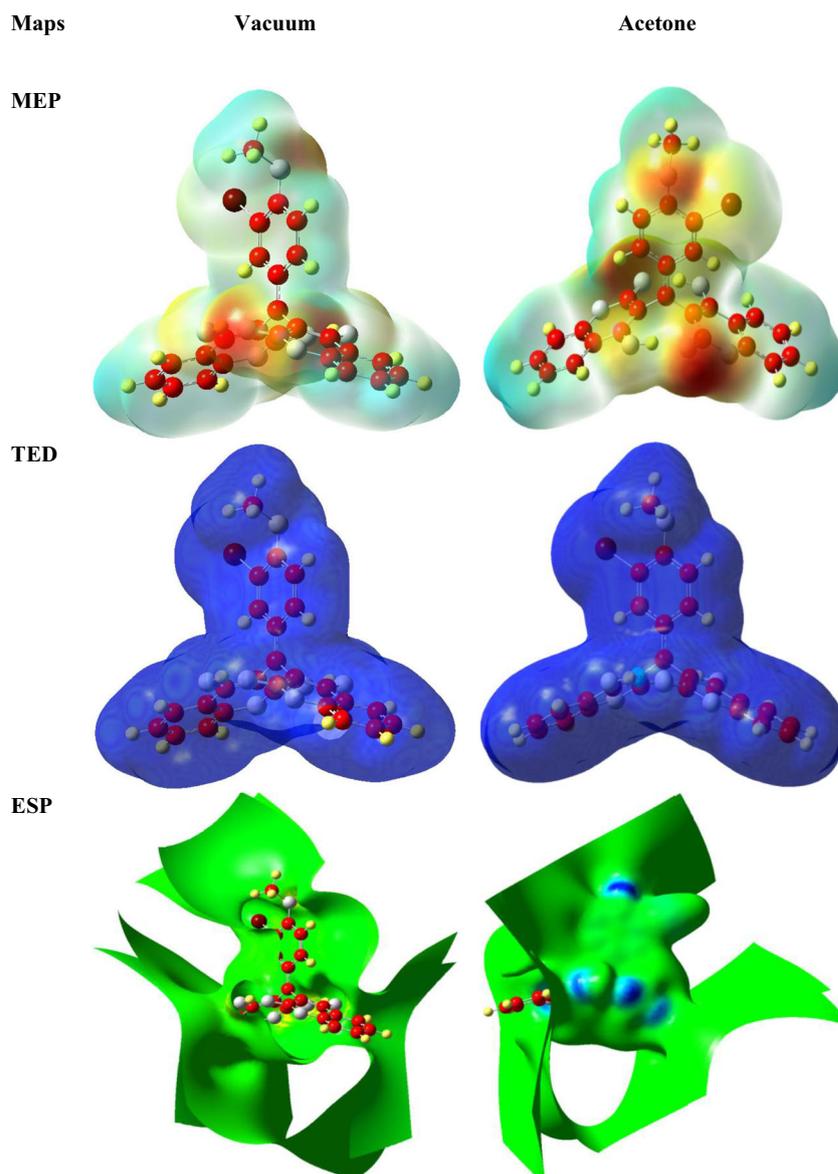
CIE Color Space Chromaticity, Coordinate, and Color Purity

The organic semiconductors are receiving great demand for designing organic light emitting diodes (OLED), polymer light-emitting diodes (PLEDs) and display device application, the advancement will create a fundamental cutting edge for the development showcases and the lighting in future. Therefore, it is important to estimate the characteristics of color emission. In order to determine the CIE color coordinate and color purity of the 3-BMH molecule, The Commission Internationale de l'Eclairage (CIE) color coordinate values have been determined by using Osram Sylvania CIE co-ordinates software [Ref OSARM]. This system consists of three primary color stimuli symbolized by X, Y and Z tristimulus integrals

$$x = \frac{X}{X + Y + Z} \tag{25}$$

$$y = \frac{Y}{X + Y + Z} \tag{26}$$

Fig. 10 HOMO LUMO plots of 3-BMH in acetone solvent

HOMO

Eg = -5.51

ΔEg = 3.39 eV

LUMO

Eg = -1.61

Fig. 11 MEP, TED, and ESP
maps of 3-BMH in
acetone solvent

| Maps | Vacuum | Acetone |

MEP

TED

ESP

Where,

$$X = \sum_{190}^{750} SPD(\lambda)\bar{x}(\lambda)d\lambda$$

$$Y = \sum_{190}^{750} SPD(\lambda)\bar{y}(\lambda)d\lambda$$

$$Z = \sum_{190}^{750} SPD(\lambda)\bar{z}(\lambda)d\lambda$$

Hence, it is clear from Fig. 12 the CIE color coordinates will lie in the deep blue region for all the solvents studied in this article, the corresponding X and Y coordinates values are tabulated in Table 7. It is found that 3-BMH showed color coordinate x = 0.14 → 0.16 and y = 0.08 → 0.31. Because of an electron withdrawing

strength of 1-bromo-2-methoxybenzene emission tuning is more highlighted. x and y chromacity values of 3-BMH in all solvents are nearly well matched to National television standard committee system (NTSC) for the ideal blue chromacity coordinate (0.14, 0.08) [33]. Color correlated temperature (CCT), U′ V′ and D_{UV} these are an important aspect of color appearance how cool (bluish) or how warm (yellowish) light appearance. D_{UV} with a positive sign for above and negative sign for below the Planckian locus is defined as the distance from the test light source to the nearest point on the Planckian locus of the CIE coordinates. The CCT was determined by transforming the x, y coordinates of a light source to U′V′, of the Planckian locus by using the following equations.
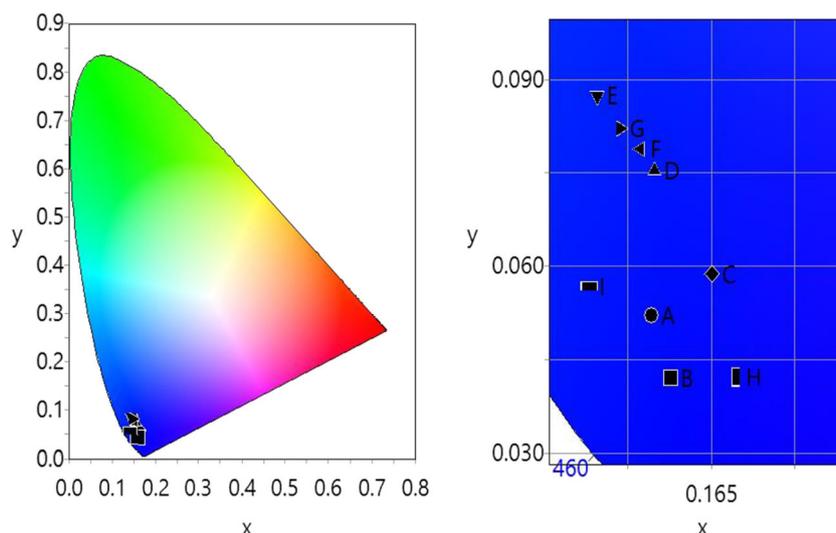
Fig. 12 CIE color coordinate spectra of 3-BMH in all studied solvents

$$U' = \frac{4x}{-2x + 12y + 3} \qquad (27)$$

$$V' = \frac{9y}{-2x + 12y + 3} \qquad (28)$$

The CCT values of 3-BMH in all solvents are found to be 4267 to 5587 K (Table 7) and shown in Fig. 13. Therefore, the 3-BMH was highly useful for the production of artificial blue light to be similar to those natural blue light simulates the natural color of daylight applications. The Du'v' output indicates error between the test lamp CCT and 3-BMH CCT as computed by software [52], so our results are considered as acceptable Du'v' errors. Color rendering index (CRI) is the quantitative measurement of the capability of a light source to reproduce the colors of different objects truly in comparison with natural light or an ideal source. The general color rendering index (CRI) is given by

$$CRI = \frac{1}{8}\sum_{i=1}^{8} R_i \qquad (29)$$

The detailed calculation of R_i (special color rendering index) was given by Aritra Ghosh et al. [64]. The performance of 3-BMH in all solvents of different polarities have high CRI values which are in greater average or equal to 87% (Table 7). This result can be concluded that higher achievable CRI values also offers higher CCT values for interior light applications [65–68]. Also, the color purity is one of the major parameters in order to estimate the percentage of color purity of the studied molecule in this work for OLED's and display application. The color purity is calculated by the equation used below

$$Color\ purity = \frac{\sqrt{(x-x_1)^2 + (y-y_1)^2}}{\sqrt{(x_2-x_1)^2 + (y_2-y_1)^2}} \times 100\% \qquad (30)$$

Solvents	CIE Coordinate		U′	V′	CCT (K)	D$_{U'V'}$	CRI	Color Purity in %
	X	Y						
Cyclohexane	0.15423	0.05214	0.1860	0.1915	4787	−0.2542	92	93.4
Hexadecane	0.15785	0.04213	0.1979	0.1889	4267	−0.2773	88	94.6
1,4-Dioxane	0.16521	0.05879	0.1958	0.2208	4703	−0.2394	78	89.8
Ethyl acetate	0.15487	0.07546	0.1723	0.1889	5587	−0.2069	84	89.0
Propanol	0.14456	0.08752	0.1537	0.2094	5558	−0.1881	90	89.8
Acetone	0.15231	0.07895	0.1672	0.1951	5238	−0.2010	87	89.1
Ethanol	0.14872	0.08213	0.1613	0.2004	4054	−0.1961	84	89.5
Methanol	0.16952	0.04215	0.2141	0.2198	4993	−0.2779	92	92.4
Dimethyl sulfoxide	0.14321	0.05678	0.1687	0.1905	4554	−0.2454	88	95.1

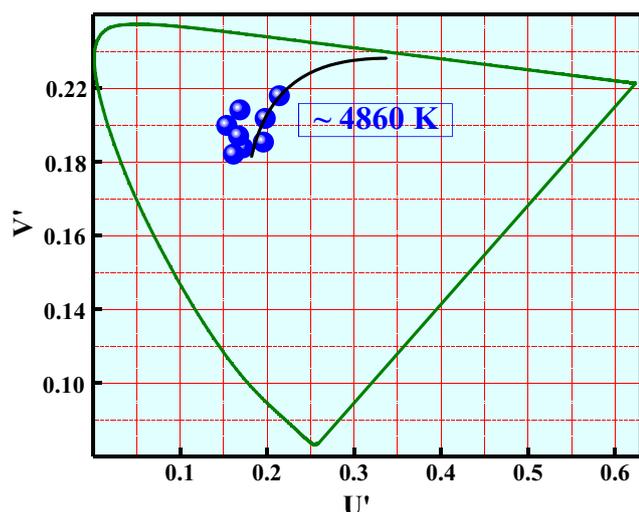**Table 7** Photometric parameters of 3-BMH in all studied solvents

Fig. 13 CCT spectra of 3-BMH in all studied solvents

Where, (x, y) are CIE chromaticity coordinate values of the studied compound, (x_1, y_1) is the color coordinate of white illumination and (x_2, y_2) is the CIE coordinate of the dominant emission wavelength. In this report the $(x_1, y_1) = (0.310, 0.316)$, $(x_2, y_2) = (0.14, 0.08)$, color purity and the (x, y) values are presented in Table 7. From Table 7 it shows the color purity percentage at an excitation wavelength of 320 nm for all studied solvents. It is found that 3-BMH showed color coordinate varies from x = 0.14 → 0.16 and y = 0.04 → 0.08. Because of an electron withdrawing strength of 1-bromo-2-methoxybenzene emission tuning is more highlighted.

Conclusions

In this present work, we have presented the experimental and theoretical determination of dipole moment of the synthesized derivative 3-BMH, the ground and excited state dipole moment have been estimated by different solvatochromic shift methods, from this it can be concluded that the excited state dipole moment is higher than the ground state dipole moment, which clearly confirms that the studied molecule is more polar in the excited state than those in the ground state. The electronic absorption and emission spectra confirm that the excited state is populated directly in nonpolar, protic and aprotic solvents. The theoretical and experimental bandgap studies confirm that the obtained bandgap value of studied 3-BMH molecule is found to be 3.41 eV for experimentally and 3.8 eV for theoretically (in average for all studied solvents) in which the obtained results are in good agreement with semiconductor bandgap values. Further, the quantum chemical investigation was performed in order to estimate the size, shape, the location of electrophilic and nucleophilic sites, polarity and charge density of molecule, distribution of charge in 3D successfully. We also report on CIE color purity, color correlated

temperature and color rendering Index of 3-BMH compound dissolved in different solvents to understand the photometric properties. To this end, the 3-BMH in all studied solvents exhibited deep blue color (x = 0.14, y = 0.08) and is a promising material for optoelectronic applications.

References

1. Liu X, Cole JM, Waddell PG, Lin TC, Radia J, Zeidler A (2012) Molecular origins of optoelectronic properties in coumarin dyes: toward designer solar cell and laser applications. J Phys Chem A 116:727–737. https://doi.org/10.1021/jp209925y
2. Ammar H, Fery-Forgues S, El Gharbi R (2003) UV/Vis absorption and fluorescence spectroscopic study of novel symmetrical biscoumarin dyes. Dyes Pigments 57:259–265. https://doi.org/10.1016/S0143-7208(03)00028-7
3. Xin JJ, Li J, Zhang ZD, Hu XB, Li MK (2015) Biscoumarin derivatives: synthesis, crystal structure, theoretical studies and induced apoptosis activity on bladder urothelial cancer cell. J Mol Struct 1084:200–206. https://doi.org/10.1016/j.molstruc.2014.12.024
4. Siddiqui ZN, Farooq F (2011) Zn(proline)2: a novel catalyst for the synthesis of dicoumarols. Catal Sci Technol 1:810. https://doi.org/10.1039/c1cy00110h
5. Li J, Lv CW, Li XJ, Qu D, Hou Z, Jia M, Luo XX, Li X, Li MK (2015) Synthesis of biscoumarin and dihydropyran derivatives and evaluation of their antibacterial activity. Molecules 20:17469–17482. https://doi.org/10.3390/molecules200917469
6. Chauthe SK, Mahajan S, Rachamalla M, Tikoo K, Singh IP (2015) Synthesis and evaluation of linear furanocoumarins as potential anti-breast and anti-prostate cancer agents. Med Chem Res 24:2476–2484. https://doi.org/10.1007/s00044-014-1312-6
7. Onishi A, Sugiyama D, Kumagai S, Morinobu A (2013) Cancer incidence in systemic sclerosis: meta-analysis of population-based cohort studies. Arthritis Rheum 65:1913–1921. https://doi.org/10.1002/art.37969
8. Ammar H, Abid S, Fery-Forgues S (2008) Synthesis and spectroscopic study of new biscoumarin dyes based on 7-(4-methylcoumarinyl) diesters. Dyes Pigments 78:1–7. https://doi.org/10.1016/j.dyepig.2007.09.008
9. Gedye R, Smith F, Westaway K, Ali H, Baldisera L, Laberge L, Rousell J (1986) The use of microwave ovens for rapid organic synthesis. Tetrahedron Lett 27:279–282. https://doi.org/10.1016/S0040-4039(00)83996-9
10. Moog RS, Kim DD, Oberle JJ, Ostrowski SG (2004) Solvent effects on electronic transitions of highly dipolar dyes: a comparison of three approaches. J Phys Chem A 108:9294–9301. https://doi.org/10.1021/jp0486088
11. Nolan KA, Doncaster JR, Dunstan MS, Scott KA, Frenkel AD, Siegel D, Ross D, Barnes J, Levy C, Leys D, Whitehead RC, Stratford IJ, Bryce RA (2009) Synthesis and biological evaluation of coumarin-based inhibitors of NAD(P)H: Quinone oxidoreductase-1 (NQO1). J Med Chem 52:7142–7156. https://doi.org/10.1021/jm9011609
12. Manjappa KB, Jhang WF, Huang SY, Yang DY (2014) Microwave-promoted, metal- and catalyst-free decarboxylative α,β-difunctionlization of secondary amino acids via pseudo-four-component reactions. Org Lett 16:5690–5693. https://doi.org/10.1021/ol5027574

13. Siddiqui ZN, Khan T (2013) Sulfuric acid-modified PEG-6000 (PEG-OSO3H): a biodegradable, reusable solid acid catalyst for highly efficient and eco-friendly synthesis of novel bis-Knoevenagel products under solvent-free conditions. Tetrahedron Lett 54:3759–3764. https://doi.org/10.1016/j.tetlet.2013.05.012

14. Díaz MS, Freile ML, Gutiérrez MI (2009) Solvent effect on the UV/Vis absorption and fluorescence spectroscopic properties of berberine. Photochem Photobiol Sci 8:970. https://doi.org/10.1039/b822363g

15. Nowak K (2014) A solvatochromic study of N-[4-(9-acridinylamino)-3-methoxyphenyl]methanesulfonamide hydrochloride: an experimental and theoretical approach. Spectrochim Acta Part A Mol Biomol Spectrosc 130:208–213. https://doi.org/10.1016/J.SAA.2014.03.004

16. Warde U, Sekar N (2017) Solvatochromic benzo [h] coumarins : synthesis , solvatochromism , NLO and DFT study. Opt Mater (Amst) 72:346–358. https://doi.org/10.1016/j.optmat.2017.06.027

17. Mande P, Mathew E, Chitrambalam S, Joe IH, Sekar N (2017) NLO properties of 1, 4-naphthoquinone, Juglone and Lawsone by DFT and Z-scan technique – a detailed study. Opt Mater (Amst) 72:549–558. https://doi.org/10.1016/J.OPTMAT.2017.06.058

18. Gülseven Sıdır Y, Sıdır İ, Berber H, Türkoğlu G (2014) Solvatochromic behavior and electronic structure of some symmetric 2-aminophenol Schiff base derivatives. J Mol Liq 199:57–66. https://doi.org/10.1016/J.MOLLIQ.2014.08.018

19. Joshi S, Bhattacharjee R, Varma YT, Pant DD (2013) Estimation of ground and excited state dipole moments of quinidine and quinidine dication: experimental and numerical methods. J Mol Liq 179:88–93. https://doi.org/10.1016/J.MOLLIQ.2012.11.023

20. Sidir I, Gülseven Sidir Y, Demiray F, Berber H (2014) Estimation of ground and excited states dipole moments of α-hydroxy phenyl hydrazone derivatives: experimental and quantum chemical methods. J Mol Liq 197:386–394. https://doi.org/10.1016/j.molliq.2014.06.001

21. Joshi S, Bhattacharjee R, Sakhuja R, Pant DD (2015) Estimation of ground and excited-state dipole moments of synthesized coumarin derivative , (S) - (1- ((7-hydroxy-2-oxo-2 H -chromen-4-yl) cabonylamino) -3-phenylpropanoate from a solvatochromic shift and theoretical methods. J Mol Liq 209:219–223. https://doi.org/10.1016/j.molliq.2015.05.053

22. Margar SN, Rhyman L, Ramasami P, Sekar N (2016) Fluorescent difluoroboron-curcumin analogs: an investigation of the electronic structures and photophysical properties. Spectrochim Acta Part A Mol Biomol Spectrosc 152:241–251. https://doi.org/10.1016/J.SAA.2015.07.064

23. Tathe AB, Sekar N (2016) NLOphoric red emitting Bis Coumarins with O-BF2-O core - synthesis, Photophysical properties and DFT studies. J Fluoresc 26:471–486. https://doi.org/10.1007/s10895-015-1733-8

24. Erande Y, Sreenath MC, Chitrambalam S, Joe IH, Sekar N (2017) Spectroscopic , DFT and Z-scan supported investigation of dicyanoisophorone based push-pull NLOphoric styryl dyes. Opt Mater (Amst) 66:494–511. https://doi.org/10.1016/j.optmat.2017.03.005

25. Guggemos N, Slavíček P, Kresin VV (2015) Electric dipole moments of Nanosolvated acid molecules in water clusters. Phys Rev Lett 114:043401. https://doi.org/10.1103/PhysRevLett.114.043401

26. Raikar US, Renuka CG, Nadaf YF, Mulimani BG (2006) Steady-state, time-resolved fluorescence polarization behaviour and determination of dipole moments of coumarin laser dye. J Mol Struct 787:127–130

27. Sıdır YG, Sıdır İ (2015) Solvatochromic fluorescence of 4-alkoxybenzoic acid liquid crystals: ground and excited state dipole moments of monomer and dimer structures determined by solvatochromic shift methods. J Mol Liq 211:591–603. https://doi.org/10.1016/j.molliq.2015.07.053

28. Renuka CG, Shivashankar K, Boregowda P, Bellad SS, Muregendrappa MV, Nadaf YF (2017) An experimental and computational study of 2-(3-Oxo-3H-benzo[f] chromen-1-ylmethoxy)-benzoic acid methyl Ester. J Solut Chem 46:1535–1555. https://doi.org/10.1007/s10953-017-0661-4

29. Goel A, Kumar V, Singh SP, Sharma A, Prakash S, Singh C, Anand RS (2012) Non-aggregating solvatochromic bipolar benzo[f]quinolines and benzo[a]acridines for organic electronics. J Mater Chem 22:14880. https://doi.org/10.1039/c2jm31052j

30. Singh V, Mishra AK (2016) White light emission from a mixture of pomegranate extract and carbon nanoparticles obtained from the extract. J Mater Chem C 4:3131–3137. https://doi.org/10.1039/c6tc00480f

31. Chang DW, Ko S-J, Kim JY, Dai L, Baek JB (2012) Multifunctional quinoxaline containing small molecules with multiple electron-donating moieties: Solvatochromic and optoelectronic properties. Synth Met 162:1169–1176. https://doi.org/10.1016/J.SYNTHMET.2012.04.016

32. Zampetti A, Minotto A, Squeo BM, Gregoriou VG, Allard S, Scherf U, Chochos CL, Cacialli F (2017) Highly efficient solid-state near-infrared organic light-emitting diodes incorporating A-D-A dyes based on α,β-unsubstituted "bODIPY" moieties. Sci Rep 7:1–7. https://doi.org/10.1038/s41598-017-01785-2

33. Kumar S, Puttaraju B, Patil S (2016) A deep-blue electroluminescent device based on a Coumarin derivative. Chempluschem 81:384–390. https://doi.org/10.1002/cplu.201500572

34. Alphonse R, Varghese A, George L, Nizam A (2016) Estimation of ground state and excited state dipole moments of a novel Schiff base derivative containing 1, 2, 4-triazole nucleus by solvatochromic method. J Mol Liq 215:387–395. https://doi.org/10.1016/j.molliq.2015.12.050

35. Panicker CY, Varghese HT, Nayak PS, Narayana B, Sarojini BK, Fun HK, War JA, Srivastava SK, van Alsenoy C (2015) Infrared spectrum, NBO, HOMO-LUMO, MEP and molecular docking studies (2E)-3-(3-nitrophenyl)-1-[4-piperidin-1-yl]prop-2-en-1-one. Spectrochim Acta - Part A Mol Biomol Spectrosc 148:18–28. https://doi.org/10.1016/j.saa.2015.03.065

36. Frisch MJ, Trucks GW, Schlegel HB, Scuseria GE, Robb MA, Cheeseman JR, Scalmani G, Barone V, Mennucci B, Petersson GA, Nakatsuji H, Caricato M, Li X, Hratchian HP, Izmaylov AF, Bloino J, Zheng G, Sonnenberg JL, Hada M, Ehara M, Toyota K, Fukuda R, Hasegawa J, Ishida M, Nakajima T, Honda Y, Kitao O, Nakai H, Vreven T, Montgomery JA, Jr., Peralta JE, Ogliaro F, Bearpark M, Heyd JJ, Brothers E, Kudin KN, Staroverov VN, Kobayashi R, Normand J, Raghavachari K, Rendell A, Burant JC, Iyengar SS, Tomasi J, Cossi M, Rega N, Millam JM, Klene M, Knox JE, Cross JB, Bakken V, Adamo C, Jaramillo J, Gomperts R, Stratmann RE, Yazyev O, Austin AJ, Cammi R, Pomelli C, Ochterski JW, Martin RL, Morokuma K, Zakrzewski VG, Voth GA, Salvador P, Dannenberg JJ, Dapprich S, Daniels AD, Farkas O, Foresman JB, Ortiz JV, Cioslowski J, Fox DJD (2009) Gaussian, Inc., Wallingford

37. Brout R, Thomas H (1967) Molecular field theory, the Onsager reaction field and the spherical model. Phys Phys Fiz 3:317–329. https://doi.org/10.1103/PhysicsPhysiqueFizika.3.317

38. Kamlet MJ, Abboud JLM, Taft RW (2007) An Examination of Linear Solvation Energy Relationships. John Wiley & Sons, Ltd, pp 485–630

39. Kamlet MJ, Abboud JL, Taft RW (1977) The Solvatochromic comparison method. 6. The π* scale of solvent Polarities1. J Am Chem Soc 99:6027–6038. https://doi.org/10.1021/ja00460a031

40. Kamlet MJ, Abboud JLM, Abraham MH, Taft RW (1983) Linear solvation energy relationships. 23. A comprehensive collection of the solvatochromic parameters, .Pi.*, .Alpha., and .Beta., and some methods for simplifying the generalized solvatochromic equation. J Org Chem 48:2877–2887. https://doi.org/10.1021/jo00165a018

41. Spektroskopiya NB-O i, 1964 undefined Universal intermolecular interactions and their effect on the position of the electronic spectra of molecules in 2-component solutions. 7. Theory (general. MEZHDUNARODNAYA Kn 39 …

42. Mataga N, Kaifu Y, Koizumi M (1956) Solvent effects upon fluorescence spectra and the Dipolemoments of excited molecules. Bull Chem Soc Jpn 29:465–470. https://doi.org/10.1246/bcsj.29.465

43. McRae EG (1954) Theory of solvent effects on molecular electronic spectra. Frequency shifts. J Phys Chem 61:1957–1572. https://doi.org/10.1021/j150551a012

44. Suppan P (1983) Excited-state dipole moments from absorption/fluorescence solvatochromic ratios. Chem Phys Lett 94:272–275. https://doi.org/10.1016/0009-2614(83)87086-9

45. Edward JT (1970) Molecular volumes and the stokes-Einstein equation, vol 47, pp 261–270

46. Li Y, Scales N, Blankenship RE, Willows RD, Chen M (2012) Extinction coefficient for red-shifted chlorophylls: chlorophyll d and chlorophyll f. Biochim Biophys Acta Bioenerg 1817:1292–1298. https://doi.org/10.1016/J.BBABIO.2012.02.026

47. Y TV, Agarwal DS, Sarmah A et al (2017) Solvent effects on the absorption and emission spectra of novel (E)-4-((4-(heptyloxy)phenyl)diazenyl)benzyl (((9H-fluoren-9-yl)methoxy)carbonyl)-d-alaninate (Fmoc-al-az): determination of dipole moment by experimental and theoretical study. J Mol Struct 1129:248–255. https://doi.org/10.1016/j.molstruc.2016.09.078

48. Baumann R, Ferrante C, Kneuper E, Deeg FW, Bräuchle C (2003) Influence of confinement on the solvation and rotational dynamics of coumarin 153 in ethanol. J Phys Chem A 107:2422–2430. https://doi.org/10.1021/jp027172y

49. Sıdır İ, Sıdır YG, Berber H, Demiray F (2015) Emerging ground and excited state dipole moments and external electric field effect on electronic structure. A solvatochromism and theoretical study on 2-((phenylimino)methyl)phenol derivatives. J Mol Liq 206:56–67. https://doi.org/10.1016/j.molliq.2015.01.056

50. Sıdır İ, Gülseven Sıdır Y (2015) Estimation of ground and excited state dipole moments of oil red O by solvatochromic shift methods. Spectrochim Acta Part A Mol Biomol Spectrosc 135:560–567. https://doi.org/10.1016/j.saa.2014.07.049

51. Luo Q, Zhang H, Zhao Y, Wang J, Yu T (2018) Synthesis and characterization of 9,10-[di-p-(7-diethylamino- coumarin-3-yl)thiopheneyl]anthracene as fluorescent material. J Sulfur Chem 39:89–98. https://doi.org/10.1080/17415993.2017.1391813

52. Sıdır YG, Sıdır İ (2012) Solvent effect on the absorption and fluorescence spectra of 7-acetoxy-6-(2,3-dibromopropyl)-4,8-dimethylcoumarin: determination of ground and excited state dipole moments. Spectrochim Acta Part A Mol Biomol Spectrosc 102:286–296. https://doi.org/10.1016/j.saa.2012.10.018

53. Y TV, Joshi S, Pant DD (2013) Solvatochromatic shift of absorption and fl uorescence spectra of 6-methoxyquinoline : estimation of ground and excited state dipole moments. J Mol Liq 179:7–11. https://doi.org/10.1016/j.molliq.2012.11.024

54. Varma YT, Pant DD (2016) Interaction of 6-methoxyquinoline with anionic sodium dodecylsulfate micelles: Photophysics and rotational relaxation dynamics at different pH. Spectrochim Acta - Part A

55. Mol Biomol Spectrosc 158:9–17. https://doi.org/10.1016/j.saa.2016.01.004

55. Riedel F, Spange S (2012) Solvatochromism of catechol derivatives - Solute/solvent interactions. J Phys Org Chem 25:1261–1268. https://doi.org/10.1002/poc.3003

56. Miotke M (2017) Solvatochromism of antiinflammatory drug – naproxen sodium Solvatochromism of antiinflammatory drug – naproxen sodium. J Mol Liq 230:129–136. https://doi.org/10.1016/j.molliq.2016.12.094

57. Renuka CG, Shivashankar K, Boregowda P, Bellad SS, Muregendrappa MV, Nadaf YF (2017) An experimental and computational study of 2- (3-Oxo-. J Solut Chem 46:1535–1555. https://doi.org/10.1007/s10953-017-0661-4

58. Pramod AG, Renuka CG, Shivashankar K et al (2018) Solvent influence on the photophysical properties of 4-(2-Oxo-2H-benzo[h]chromen-4-ylmethoxy)-benzaldehyde. In: AIP conference proceedings. AIP Publishing LLC, p 130001

59. Tej Varma Y, Agarwal DS, Sarmah A et al (2017) Solvent effects on the absorption and emission spectra of novel (E)-4-((4-(heptyloxy)phenyl)diazenyl)benzyl (((9H-fluoren-9-yl)methoxy)carbonyl)-D-alaninate (Fmoc-al-az): determination of dipole moment by experimental and theoretical study. J Mol Struct 1129:248–255. https://doi.org/10.1016/j.molstruc.2016.09.078

60. Khatir-Hamdi N, Makhloufi-Chebli M, Grib H et al (2019) Synthesis DFT/TD-DFT theoretical studies and experimental solvatochromic shift methods on determination of ground and excited state dipole moments of 3-(2-hydroxybenzoyl) coumarins. J Mol Struct 1175:811–820. https://doi.org/10.1016/j.molstruc.2018.08.039

61. Mott NF, Davis EA (2012) Electronic processes in non-crystalline materials. Oxford University Press

62. Sıdır İ, Sıdır YG, Berber H, Demiray F (2019) Electronic structure and optical properties of Schiff base hydrazone derivatives by solution technique for optoelectronic devices: synthesis, experiment and quantum chemical investigation. J Mol Struct 1176:31–46. https://doi.org/10.1016/J.MOLSTRUC.2018.08.067

63. Umarani P, Thiruvalluvar A, Raja CR (2018) A critical study of crystal structure, N—H—Br interaction, effect of charge transfer on third-order nonlinear optical properties and optical limiting behaviour of a new crystal: (4-Methoxyphenyl) methanaminium bromide. J Mol Struct 1173:822–832. https://doi.org/10.1016/j.molstruc.2018.07.043

64. Ghosh A, Selvaraj P, Sundaram S, Mallick TK (2018) The colour rendering index and correlated colour temperature of dye-sensitized solar cell for adaptive glazing application. Sol Energy 163:537–544. https://doi.org/10.1016/J.SOLENER.2018.02.021

65. Houser K, Mossman M, Smet K, Whitehead L (2016) Tutorial: color rendering and its applications in lighting. LEUKOS - J Illum Eng Soc North Am 12:7–26. https://doi.org/10.1080/15502724.2014.989802

66. Li C, Cui G, Melgosa M, Ruan X, Zhang Y, Ma L, Xiao K, Luo MR (2016) Accurate method for computing correlated color temperature. Opt Express 24:14066. https://doi.org/10.1364/OE.24.014066

67. Zikriya M, Nadaf YF, Manjunath C, Renuka CG (2018) Microstructural and optical properties of rare earth ions doped TiO2 for potential white LED applications. J Mater Sci Mater Electron 29:16824–16835. https://doi.org/10.1007/s10854-018-9777-6

68. McCamy CS (1992) Correlated color temperature as an explicit function of chromaticity coordinates. Color Res Appl 17:142–144. https://doi.org/10.1002/col.5080170211